Spatiotemporal analyses of soil moisture from point to footprint scale in two different hydroclimatic regions

Champa Joshi,[1] Binayak P. Mohanty,[1] Jennifer M. Jacobs,[2] and Amor V. M. Ines[1,3]

Received 11 December 2009; revised 27 July 2010; accepted 25 October 2010; published 25 January 2011

[1] This paper presents time stability analyses of soil moisture at different spatial measurement support scales (point scale and airborne remote sensing (RS) footprint scale 800 m × 800 m) in two different hydroclimatic regions. The data used in the analyses consist of in situ and passive microwave remotely sensed soil moisture data from the Southern Great Plains Hydrology Experiments 1997 and 1999 (SGP97 and SGP99) conducted in the Little Washita (LW) watershed, Oklahoma, and the Soil Moisture Experiments 2002 and 2005 (SMEX02 and SMEX05) in the Walnut Creek (WC) watershed, Iowa. Results show that in both the regions soil properties (i.e., percent silt, percent sand, and soil texture) and topography (elevation and slope) are significant physical controls jointly affecting the spatiotemporal evolution and time stability of soil moisture at both point and footprint scales. In Iowa, using point-scale soil moisture measurements, the WC11 field was found to be more time stable (TS) than the WC12 field. The common TS points using data across the 3 year period (2002–2005) were mostly located at moderate to high elevations in both the fields. Furthermore, the soil texture at these locations consists of either loam or clay loam soil. Drainage features and cropping practices also affected the field-scale soil moisture variability in the WC fields. In Oklahoma, the field having a flat topography (LW21) showed the worst TS features compared to the fields having gently rolling topography (LW03 and LW13). The LW13 field (silt loam) exhibited better time stability than the LW03 field (sandy loam) and the LW21 field (silt loam). At the RS footprint scale, in Iowa, the analysis of variance (ANOVA) tests show that the percent clay and percent sand are better able to discern the TS features of the footprints compared to the soil texture. The best soil indicator of soil moisture time stability is the loam soil texture. Furthermore, the hilltops (slope ∼0%–0.45%) exhibited the best TS characteristics in Iowa. On the other hand, in Oklahoma, ANOVA results show that the footprints with sandy loam and loam soil texture are better indicators of the time stability phenomena. In terms of the hillslope position, footprints with mild slope (0.93%–1.85%) are the best indicators of TS footprints. Also, at both point and footprint scales in both the regions, land use–land cover type does not influence soil moisture time stability.

Citation: Joshi, C., B. P. Mohanty, J. M. Jacobs, and A. V. M. Ines (2011), Spatiotemporal analyses of soil moisture from point to footprint scale in two different hydroclimatic regions, *Water Resour. Res., 47*, W01508, doi:10.1029/2009WR009002.

1. Introduction

[2] Soil moisture is a key state variable of the hydrologic cycle. It plays a significant role in many hydrological, meteorological, and other natural processes in the land-atmosphere continuum [*Entin et al.,* 2000]. It greatly affects the partitioning of precipitation into infiltration and runoff, thereby regulating the extent of groundwater recharge and the fate and transport of contaminants both on the surface and in the subsurface. Soil moisture in the root zone is also vital for the growth and development of crops as it plays a significant role in the partitioning of the surface energy budget, hence the crop water requirements [*Grayson and Western,* 1998]. Soil moisture distribution is highly nonlinear across time and space. Various geophysical factors (e.g., soil texture, topography, land use–land cover (LULC), and weather/climate) and their interactions contribute toward the spatiotemporal evolution of soil moisture at various scales. Understanding these interactions is crucial for the characterization of soil moisture dynamics occurring in the vadose zone [*Mohanty and Skaggs,* 2001].

[3] Soil moisture can be estimated in various ways: by direct in situ methods, e.g., gravimetric sampling, neutron

[1]Department of Biological and Agricultural Engineering, Texas A&M University, College Station, Texas, USA
[2]Department of Civil Engineering, University of New Hampshire, Durham, New Hampshire, USA
[3]Now at International Research Institute for Climate and Society, Earth Institute at Columbia University, Palisades, New York, USA

0043-1397/11/2009WR009002

probe, and time domain reflectometry (TDR) [*Grayson and Western,* 1998; *Mohanty et al.,* 1998; *Famiglietti et al.,* 1999], and by indirect methods using remote sensing (RS) techniques, e.g., active [*De Troch et al.,* 1996; *Ulaby et al.,* 1996] and passive [*Jackson and Schmugge,* 1995; *Jackson and Levine,* 1996; *Schmugge,* 1998; *Jackson,* 2003; *Njoku et al.,* 2003] microwave measurements from airborne or spaceborne remote sensors. The in situ methods have small measurement support (at point scale) compared to the RS methods in which the microwave sensors provide soil moisture estimates at larger spatial scales. Passive microwave sensor penetration depths, however, are limited to the near-surface soil layers ($\sim$0–5 cm).

[4] Remote sensing of soil moisture needs to be calibrated and validated using soil moisture measurements recorded on the ground [*Yoo,* 2002]. The calibration and validation of RS products is done using footprint-scale (mean) soil moisture data obtained from ground sampling. Full validation, however, is inherently difficult because of various reasons, e.g., the mismatch in scale between in situ measurements and RS footprints (10^2–10^3 m), the limited number of ground samples per footprint, and the high spatial variability of soil moisture due to soil types, vegetation, topography, and weather/climate [*Cosh et al.,* 2004a; *Jacobs et al.*, 2004]. This RS validation problem often necessitates the identification of locations within a field or footprint that can estimate the field or footprint mean soil moisture and can retain their stability over a long period of time. These locations, referred to as time stable (TS) locations [*Vachaud et al.,* 1985; *Mohanty and Skaggs,* 2001], can be effectively used to reduce the number of in situ sampling points in designing hydrology experiments for RS validation purposes. They can also be used to estimate the average soil moisture content of large watersheds adequately [*Mohanty and Skaggs,* 2001] and help in downscaling RS soil moisture products. They are crucial for determining physical controls that can affect the soil moisture spatiotemporal variability at different scales, from point to footprint scales [*Mohanty et al.,* 2000; *Cosh et al.,* 2004a; *Jacobs et al.*, 2004].

[5] *Vachaud et al.* [1985] introduced the concept of time stability by conducting a soil moisture experiment in a 2000 m^2 grass field having alluvial soil in France and further corroborated the concept by testing it in two separate regions. *Kachanoski and Dejong* [1988] examined the temporal persistence of a spatial pattern of soil moisture as a function of spatial scale using the spatial coherency analysis method. Their study area consisted of a small grass field with rolling topography located in Saskatchewan, Canada. *Grayson and Western* [1998] used four sets of soil moisture measurements made over depths from 30 to 120 cm to determine TS locations in three different catchments: Tarrawara and Lockyersleigh (in Australia) and R5-Chickasha (United States). The catchments range in size from 10.5 ha to 27 km^2 and have significant relief. *Mohanty and Skaggs* [2001] studied the effects of soil type, slope, and vegetation on the spatiotemporal evolution and time stability of soil moisture using theta probe and RS data in three different fields in the Southern Great Plains (SGP) region. They found that the sandy loam field exhibited better TS features compared to the other two fields containing silt loam soils. They also observed that the field having flat topography had the worst time stability compared to the two fields with gently rolling topography. *Martinez-Fernandez and Ceballos* [2003] determined the TS characteristics in an area of 1285 km^2 receiving uniform rainfall located in the Duero basin in Spain. According to them, the time stability of soil moisture is always higher when the soils are dry compared to when the conditions are wet. Also, the lowest temporal stability is observed during the transition period from dry to wet. They further observed that the dry locations in the field were much more time stable (at all depths, 5–100 cm) with their temporal stability within the range of 6%–9% compared to the wet locations. These dry locations have soils with higher sand fraction, and therefore, they are unable to retain water, resulting in lower moisture content values and relatively higher time stability. *Cosh et al.* [2004a] and *Jacobs et al.* [2004] investigated the time stability of the WC fields in the Walnut Creek (WC) watershed, Iowa, using in situ soil moisture data. *Cosh et al.* [2004a] derived watershed-scale mean soil moisture estimates for the validation of satellite products with small errors (3%). *Jacobs et al.* [2004] observed that locations with mild slope consistently showed TS features, while locations on hilltop and high slopes underestimated the mean field soil moisture. Using ground-based measurements from a dense network of 19 sensors distributed over a 150 km^2 semiarid region of the Walnut Gulch Experimental Watershed in southeastern Arizona, *Cosh et al.* [2008] found that much of the sensor network was time stable in estimating the watershed mean moisture content during a 3.5 year time period, from 1 March 2002 to 13 September 2005. But the mean relative difference plot obtained from the Soil Moisture Experiment 2004 (SMEX04) gravimetric soil moisture (GVSM) samples (collected during 3–26 August 2004) was not duplicated by the network mean relative difference plot. They concluded that the network does not record the surface soil moisture patterns accurately; rather, it consists of an accurate set of sample points that predict the watershed average soil moisture content. While soil type characterized by bulk density, clay, and sand content influenced 50% of the temporal stability, topographic effects were less significant. *Choi and Jacobs* [2007] studied the field-scale spatiotemporal variability of root zone soil moisture in the WC11 and WC13 fields in the WC watershed. On the basis of their analyses, they claimed that time stability of surface soil moisture measurements is a good indicator of subsurface time stability. Other studies investigating the spatiotemporal variability of surface soil moisture and its linkages with different geophysical attributes, at varying spatial scales using both ground-based and remotely sensed moisture contents in the SGP region, include the works of *Kim and Barros* [2002a, 2002b], *Cosh et al.* [2004b], *Ryu and Famiglietti* [2005], and *Famiglietti et al.* [2008].

[6] The objectives of this study are as follows. The first objective is to investigate the temporal evolution of the TS features of two footprints or fields in the WC watershed, Iowa, using ground-based soil moisture measurements obtained from the Soil Moisture Experiment campaigns in 2002 and 2005 (SMEX02 and SMEX05) and analyze whether the TS locations maintain their stability features over the 3 year period. The second objective is to study the TS characteristics of RS footprints or pixels within the WC

watershed in Iowa (during SMEX02 and SMEX05) and the Little Washita (LW) watershed in Oklahoma (during the Southern Great Plains Hydrology Experiments 1997 and 1999 (SGP97 and SGP99)) using airborne RS soil moisture data and compare the footprint-scale TS features with the ground-based soil moisture analyses to determine the common physical controls affecting the spatiotemporal evolution of soil moisture at different measurement support scales.

2. Materials and Methods

2.1. Study Regions

2.1.1. Walnut Creek Watershed, Iowa

[7] The WC watershed (Figure 1), located south of Ames, Iowa, has an area of 100 km^2. The climate of the area is mostly humid, with an average annual precipitation of 835 mm. The regional topography consists of low-relief features with poor surface drainage due to the existing prairie potholes of glacial origin. The elevation of the WC watershed ranges between 270 and 320 m. The soil texture of this region varies considerably from fine sandy loam to clay, with the majority classified as silt loam with a relatively low permeability. Mostly row type cultivation is done in this region, with corn (50%) and soybean (40%) crops dominating the land cover [*Choi and Jacobs,* 2007]. The hydrology and climate of the WC watershed and the region around Ames, Iowa, have been regularly monitored by the U.S. Department of Agriculture National Soil Tilth Laboratory over the past two decades. As such, this area has been the focus of large-scale soil moisture experiments (SMEX) since 2002. The SMEX02 field campaign was carried out from 25 June to 12 July 2002, and SMEX05 took place from 13 June to 4 July 2005. A detailed description of the two campaigns, including the objectives of the mission, experiment plan, and site description, can be found on the Agricultural Research Service Web site (http://www.ars.usda.gov/Research/docs.htm?docid=8974).

[8] Figure 1 shows the two fields, WC11 and WC12, that were selected for this spatiotemporal study. The location and significant attributes of the fields are given in Table 1. The dimension of each field is approximately 800 m × 800 m, which is similar to the footprint resolution of different airborne remote sensors (Electronically Scanned Thin Array Radiometer (ESTAR), Two-Dimensional Synthetic Aperture Radiometer (2D-STAR), and Polarimetric Scanning Radiometer (PSR)). During SMEX02, WC11 had a corn crop cover with a small patch of soybean planted near the western edge of the field. During SMEX05, the corn crop in the WC11 field was rotated with a soybean crop. The WC12 field had a tile drainage system from southwest to northeast and was planted with corn (row cultivation) during both SMEX02 and SMEX05. During SMEX02, soil moisture content was measured for 12 days at 92 points in the WC11 field and 132 points in the WC12 field (see Figure 1). Again, during the SMEX05 campaign, sampling was done at 87 points in WC11 and 64 points in WC12. Sampling points were located at nearly 30 m intervals along the four transects oriented east–west and north–south in WC11 and a single east–west and two north–south transects in WC12 (see Figure 1). During the experiments, volumetric soil moisture (VSM) contents were measured between 1100 and 1500 local time (CDST) using 6 cm long theta probes and data loggers (ML-2 probes and HH2 data loggers of Delta-T Inc., United Kingdom). The airborne PSR observations (resolution of 800 m × 800 m) were collected from 25 June to 12 July 2002 during SMEX02 (Figure 2a). However, the RS soil moisture data acquired through Airborne Polarimetric Microwave Imaging Radiometer (APMIR) during the SMEX05 campaign are not yet available in the public domain. The PSR is an airborne microwave imaging radiometer developed and operated by the National Oceanic and Atmospheric Administration (NOAA) Environmental Technology Laboratory [*Piepmeier and Gasiewski,* 2001]. *Bindlish et al.* [2005] provide a complete description of the functional operation (i.e., the flight lines and mapping specifications) of PSR during SMEX02.

2.1.2. Little Washita Watershed, Oklahoma

[9] The LW watershed (Figure 3) in Oklahoma lies in the southern part of the Great Plains of the United States. This 610 km^2 watershed is a tributary of the Washita River in southwest Oklahoma. The climate of the region is subhumid, with an average annual precipitation of 750 mm. The region has a moderately rolling topography with the elevation ranging between 321 and 459 m within the expanse of the LW watershed. Soil texture varies considerably, with large areas having both coarse and fine textures. Land cover is mostly dominated by rangeland and pasture, with significant areas having winter wheat and other crops [*Mohanty et al.,* 2002]. The LW watershed and its surrounding areas are considered to be one of the best instrumented sites in the world for surface soil moisture, hydrology, and meteorology [*Mohanty and Skaggs,* 2001]. This is the key reason for selecting this region for a series of watershed-scale soil moisture experiments, namely, SGP97 and SGP99, SMEX03, and, more recently, the Cloud and Land Surface Interaction Campaign (CLASIC) in the summer of 2007. The SGP97 soil moisture campaign took place between 18 June and 17 July 1997, and SGP99 was carried out from 8 to 21 July 1999. A detailed description of both the experiments can be found on the Agricultural Research Service Web site (http://www.ars.usda.gov/Research/docs.htm?docid=8974). The CLASIC campaign was conducted for a 3 week long period in June 2007. Details regarding CLASIC, its goals and objectives, site description, experiment plan, etc., can be found on the CLASIC Web site (http://acrf-campaign.arm.gov/clasic/).

[10] Figure 3 shows the three fields (LW03, LW13, and LW21) that were selected for our long-term soil moisture spatiotemporal variability study. The fields are approximately 800 m × 800 m, the same as the resolution of an airborne RS (ESTAR/2DSTAR) footprint. Table 2 gives the details of the geographical location and significant environmental attributes of the LW fields. LW03 and LW13 are gently rolling rangelands. LW03 is predominantly sandy loam with a few small patches of loam soil, whereas the soil texture of LW13 is mainly silt loam with a patch of loam soil. LW21 is a flat, split winter wheat–grass field with silt loam soil. During SGP97, VSM content in the 0–6 cm surface soil layer was measured daily at 49 sampling points, in a regular 7 × 7 square grid with 100 m spacing (Figure 3). In SGP97, we have, in total, 23, 24, and 17 complete sets of daily soil moisture data for fields LW03, LW13, and LW21, respectively. Furthermore, from CLASIC, we

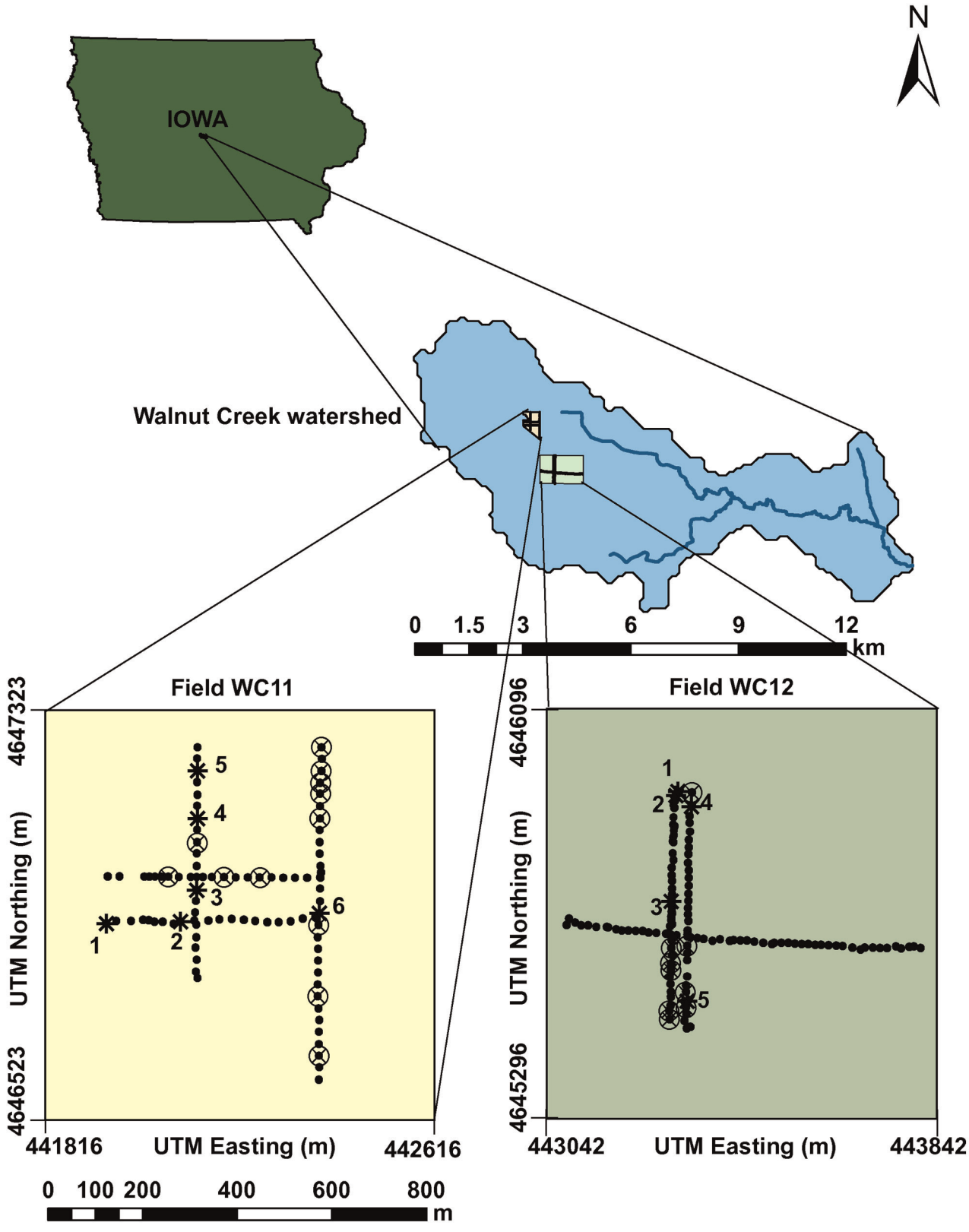

Figure 1. Sampling points in the WC fields in the Walnut Creek (WC) watershed (Iowa) during the SMEX02 and SMEX05 campaigns. All the marked locations were time stable during both SMEX02 and SMEX05 within ±10% volumetric soil moisture (VSM). Locations 1–6 in WC11 and 1–5 in WC12 (marked with an asterisk) were time stable during both SMEX02 and SMEX05 within ±5% VSM.

Table 1. Geographical Locations and Field Attributes for the WC11 and WC12 Fields in the WC Watershed, Iowa

Field	Universal Transverse Mercator Coordinates of the NE Corner of the Field	Mean Soil Texture (%)		Crop Type		Topography	Drainage Features
		Sand	Clay	SMEX02	SMEX05		
WC11	442,616E, 4,647,323N	24.5	28.6	corn (soybeans)	soybeans (corn)	hilltop and slope	no
WC12	443,842E, 4,646,096N	26.1	27.7	corn	corn	drainage features	yes

have a 10 day long data set of theta probe measured soil moisture estimates from 11 to 25 June 2007 for the LW21 field. During the SGP97 and SGP99 campaigns, a NASA P-3 aircraft based ESTAR instrument was used to measure the pixel average daily surface (0–5 cm) soil moisture contents across the entire SGP study region (Figure 4a). The ESTAR is a synthetic aperture, L band passive microwave radiometer operating at a center frequency of 1.413 GHz and a bandwidth of 20 MHz. Details about the instrument and resulting soil moisture products can be found on the Goddard Earth Sciences Data and Information Services Center Web page (http://hydrolab.arsusda.gov/sgp97/sgp97f2.pdf). For this study, the ESTAR-measured soil moisture data set is available for 16 days (18 June to 16 July 1997) during SGP97 and for 5 days (8–20 July 1999) during the SGP99 campaign.

2.2. Time Stability Analysis

[11] The time stability concept introduced by *Vachaud et al.* [1985] has been widely used to analyze the TS characteristics of soil moisture fields and determine the TS locations that are representative of the field or pixel mean soil moisture under different scenarios. According to *Vachaud et al.* [1985], time stability is the time-invariant association between spatial location and classical statistical parametric values of different soil properties. Two statistical metrics normally used to conduct the time stability analysis are the mean relative difference (equation (1)) and the root-mean-square of relative difference (equation (4)).

[12] The mean relative difference $\overline{\delta}_{i,j}$ (% vol/vol) at a sampling location i in field j is defined as

$$\overline{\delta}_{i,j} = \frac{1}{n_t}\sum_{t=1}^{n_t}\frac{\theta_{i,j,t} - \overline{\theta}_{j,t}}{\overline{\theta}_{j,t}}, \tag{1}$$

where $\overline{\theta}_{j,t}$ (% vol/vol) is the field mean soil moisture calculated as

$$\overline{\theta}_{j,t} = \frac{1}{n_{j,t}}\sum_{i=1}^{n_{j,t}}\theta_{i,j,t}. \tag{2}$$

[13] In equations (1) and (2), t is the total number of days soil sampling was done ($t = 1,2,\ldots, n_t$), and $\theta_{i,j,t}$ is the VSM content measured at location i ($i = 1,2,\ldots, n_{j,t}$) in field j at time t.

[14] The rank-ordered mean relative difference plot, with error bounds of one standard deviation of the relative difference, helps us locate the best TS positions within a field. A negative mean relative difference value signifies that the location is drier than the field-averaged soil moisture, whereas a positive value of mean relative difference indicates that the location is wetter than the field-averaged soil moisture.

[15] The variance of the relative difference for each sampling location is calculated as

$$\sigma(\delta)^2_{i,j} = \frac{1}{n_t - 1}\sum_{t=1}^{n_t}\left(\frac{\theta_{i,j,t} - \overline{\theta}_{j,t}}{\overline{\theta}_{j,t}} - \overline{\delta}_{i,j}\right)^2. \tag{3}$$

[16] Thus, the mean relative difference measures the bias of the soil moisture value at a particular sampling location, and the variance of the relative difference indicates the accuracy of that measurement. Together these two statistical metrics combine to give the root-mean-square error (RMSE) of the relative difference as

$$\mathrm{RMSE}_{i,j} = \left(\overline{\delta}^2_{i,j} + \sigma(\delta)^2_{i,j}\right)^{1/2}. \tag{4}$$

[17] Therefore, $\mathrm{RMSE}_{i,j}$ includes both bias and accuracy metrics [*Jacobs et al.,* 2004]. On the basis of the rank-ordered $\mathrm{RMSE}_{i,j}$ plot, the sampling locations having lower RMSE values are considered temporally more stable compared to the ones having higher RMSE values within a field. In short, both mean relative difference and $\mathrm{RMSE}_{i,j}$ can be used to identify the locations within a field or an RS pixel that consistently monitor the field or pixel mean soil moisture with permissible degrees of error, along with the wetter and drier points plus the extent of their variability compared to the field or pixel mean soil moisture [*Mohanty and Skaggs,* 2001].

[18] Appropriate sampling locations or RS footprints within a field or watershed having high TS features can be identified a priori on the basis of the available physical parameters (e.g., topography, soil, and vegetation) using a one-way analysis of variance (ANOVA) that tests whether statistically significant differences exist among the group mean values [*Ott*, 1997]. In a one-way ANOVA, the pooled error variance is calculated, and the resulting F statistic is used to test the null hypothesis, which states that the population means are equal. Thus, using ANOVA, we can determine if significant differences in soil moisture time stability exist among the available physical parameters, such as soil, topography, and LULC [*Jacobs et al.*, 2004].

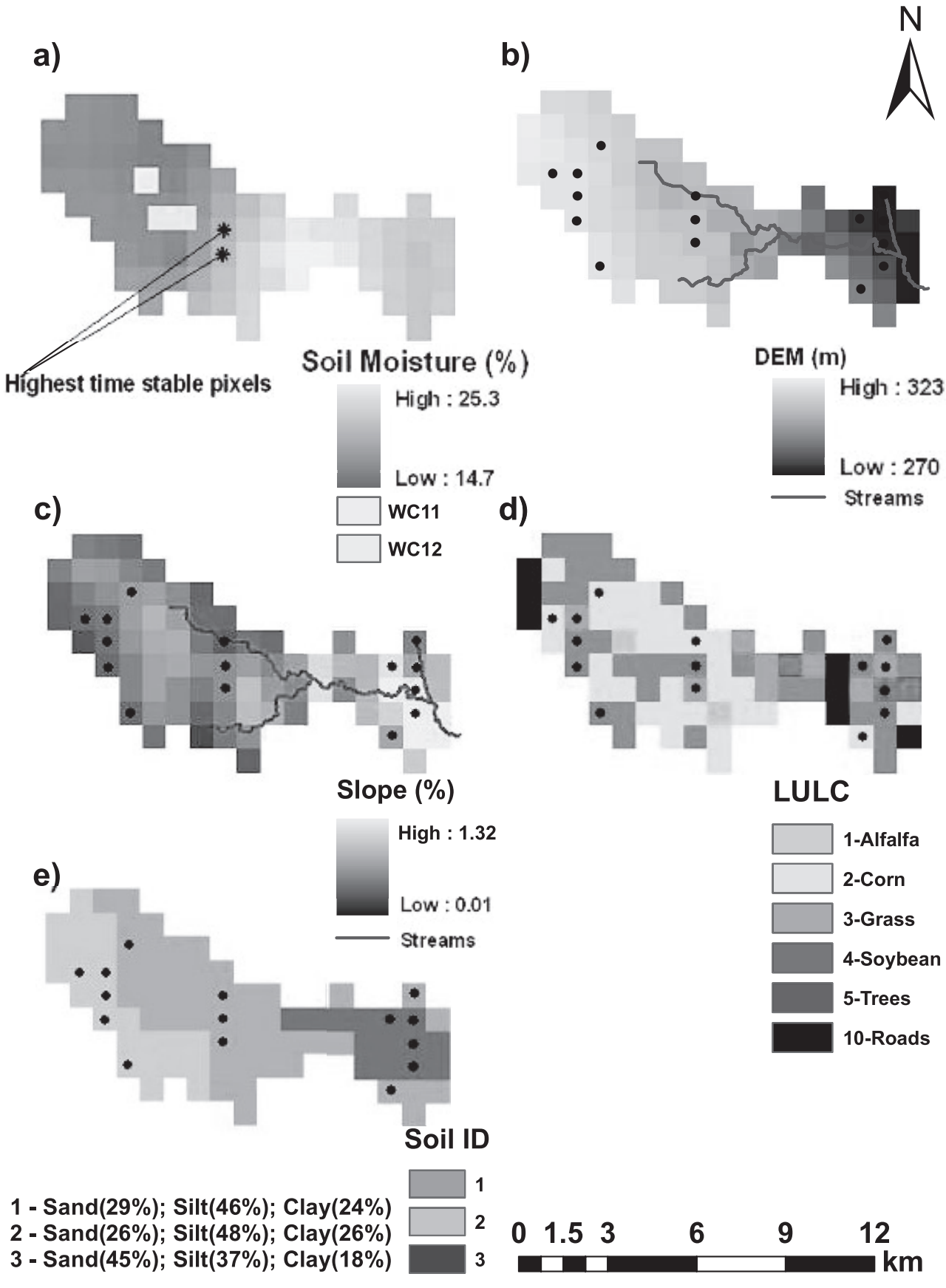
a)
b)
N
Highest time stable pixels
Soil Moisture (%)
High : 25.3
Low : 14.7
WC11
WC12
DEM (m)
High : 323
Low : 270
Streams
c)
d)
Slope (%)
High : 1.32
Low : 0.01
Streams
LULC
1-Alfalfa
2-Corn
3-Grass
4-Soybean
5-Trees
10-Roads
e)
Soil ID
1 - Sand(29%); Silt(46%); Clay(24%)
2 - Sand(26%); Silt(48%); Clay(26%)
3 - Sand(45%); Silt(37%); Clay(18%)
1
2
3
0 1.5 3 6 9 12
km

Figure 2

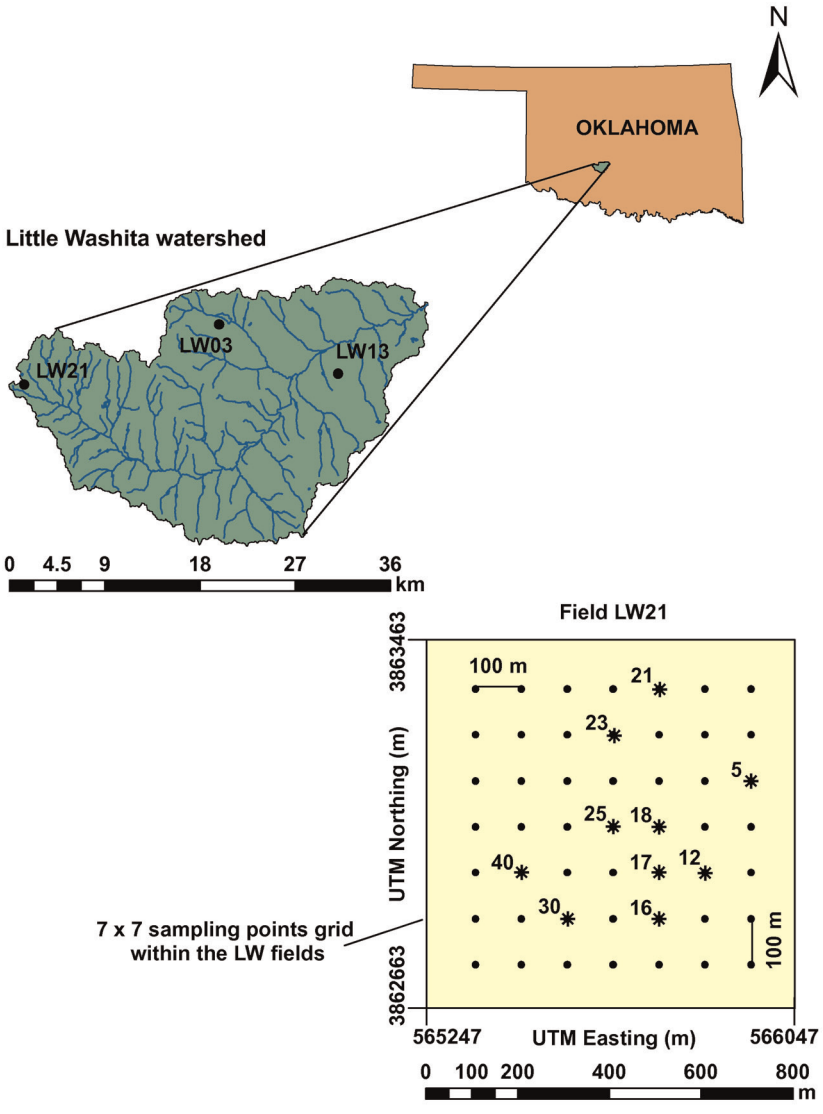

Figure 3. Sampling points grid within the LW fields in the Little Washita (LW) watershed (Oklahoma) during the SGP97 campaign. Locations marked with an asterisk in the LW21 field were time stable during both SGP97 and CLASIC.

Table 2. Geographical Locations and Field Attributes for the LW03, LW13, and LW21 Fields in the LW Watershed, Oklahoma

Field	Universal Transverse Mercator Coordinates of the NE Corner of the Field	Soil Texture	Crop Type	Topography
LW03	584,467E, 3,869,166N	sandy loam	rangeland	rolling
LW13	595,701E, 3,864,517N	silt loam	rangeland	rolling
LW21	566,047E, 3,863,463N	silt loam	wheat/grass	flat

Figure 2. The WC watershed, Iowa, (a) Polarimetric Scanning Radiometer (PSR)–derived soil moisture map of 25 June 2002 (pixels marked with an asterisk had the highest time stability with a ±0.5% bias and lowest root-mean-square error values), (b) digital elevation model (DEM), (c) slope, (d) land use–land cover (LULC) during SMEX02, and (e) soil texture map. Pixels marked with a dot are the time-stable (TS) pixels that estimated the watershed mean soil moisture within ±2% VSM.

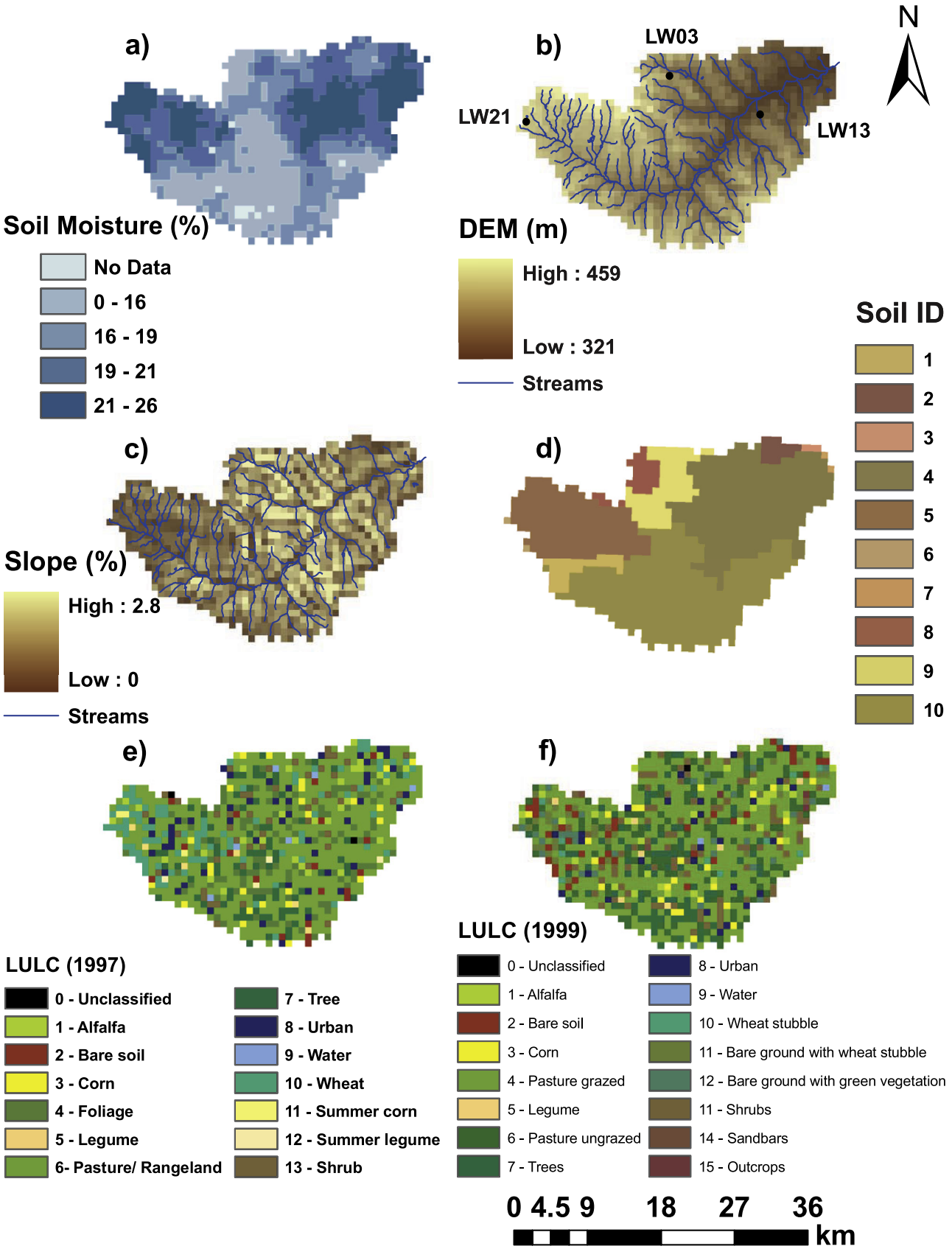

Figure 4. The LW watershed, Oklahoma, (a) Electronically Scanned Thin Array Radiometer (ESTAR)–estimated soil moisture map of 18 June 1997, (b) DEM, (c) slope, (d) soil texture map, (e) LULC cover during SGP97, and (f) LULC cover during SGP99. Soil texture corresponding to the soil ID in Figure 4d is given in Table 3.

Table 3. Percent Sand, Silt, and Clay Distribution Within the Pixels in the LW Watershed, Oklahoma[a]

Soil ID	Sand (%)	Silt (%)	Clay (%)
1	41	45	15
2	23	63	14
3	18	69	13
4	37	47	15
5	21	66	13
6	58	32	10
7	30	50	20
8	79	15	6
9	60	31	10
10	56	32	12

[a]In accordance with the legend of the soil map of the watershed in Figure 4d.

3. Results and Discussion

3.1. Walnut Creek Watershed, Iowa

3.1.1. Field-Scale Time Stability Analyses with Ground-Based Point-Scale Observations

[19] The time series of soil moisture for the WC11 and the WC12 fields in the WC watershed (Iowa) during SMEX02 and SMEX05 are shown in Figure 5. It is evident that the mean soil moisture content of field WC11 is higher than the WC12 field in both the years (2002 and 2005), similar to the findings of *Jacobs et al.* [2004] for 2002. The higher mean soil moisture of the WC11 field can be partially attributed to the higher clay (28.6%) and lower sand content (24.5%) of the field compared to the WC12 field (clay ~27.7% and sand ~26.1%). The presence of tile drains in WC12 facilitates the soil water drainage and thus contributes toward the lower mean soil moisture contents of the WC12 field. Also, the variability of soil moisture is higher in WC11 than WC12 for both SMEX02 and SMEX05. The soil moisture variability decreases immediately after a rainfall event and then increases for both fields during the drying period. The trend of soil moisture variability in WC11 is somewhat like WC12 in 2002 (Figure 5c) and less similar to WC12 in 2005. This behavior may be due to the fact that during SMEX02, both WC11 and WC12 were planted with corn, whereas during SMEX05, WC11 was planted with soybean and WC12 was planted with corn. Corn is usually a denser crop and has a higher leaf area index and stronger light extinction properties than soybean. These properties of corn fields could have caused higher transpiration loss and led to a more uniform distribution of soil moisture content with depth than the soybean fields [*Jacobs et al.,* 2004]. This may explain the difference between the soil moisture variability trends in the WC11 field during SMEX05 compared to SMEX02.

[20] Figure 6 shows the rank-ordered $\overline{\delta}_{i,j}$ values within ± 1 standard deviation along with their RMSE values for each sampling location in the WC11 and WC12 fields during SMEX02 and SMEX05. A comparison of Figures 6a–6d shows that the WC11 field maintained its higher TS characteristics and lower temporal variability compared to WC12 over a 3 year period (2002–2005). During SMEX02, out of 92 sampling locations in WC11, 32 locations (nearly 35%) captured the field mean soil moisture content within $\pm 10\%$ VSM. Approximately 44% of these 32 locations (14 out of 32 locations) captured the field mean within $\pm 5\%$ VSM. During SMEX05, approximately 35 out of 87 sampling locations (about 40%) captured the field mean soil moisture within $\pm 10\%$ VSM. About 51% of

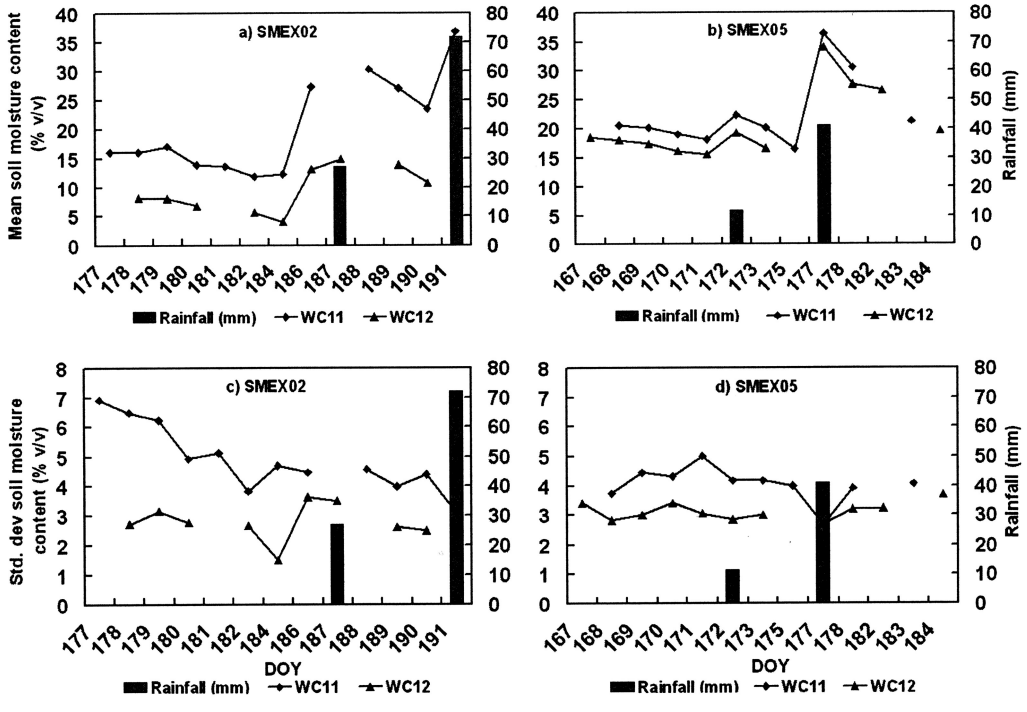

Figure 5. (a and b) Mean and (c and d) standard deviation of volumetric soil moisture content of the WC fields in the WC watershed (Iowa) during the SMEX02 and SMEX05 campaigns.

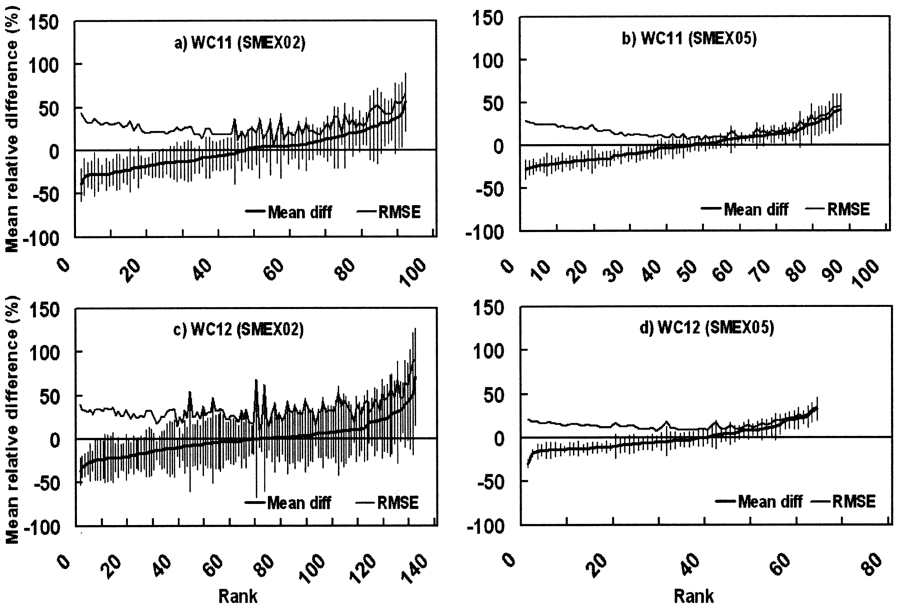

Figure 6. Rank-ordered mean relative difference with one standard deviation error bars and root-mean-square error for each sampling point in the (a and b) WC11 and (c and d) WC12 fields in the WC watershed (Iowa) during the SMEX02 and SMEX05 campaigns.

these 35 locations (i.e., 18 locations) captured the field average within ±5% VSM. Furthermore, investigation in the WC11 field showed that 18 of the 32 TS locations (56%) from SMEX02 (see Figure 1) exhibited TS features during SMEX05 as well, estimating the field mean soil moisture within ±10% VSM. Approximately 33% of these 18 repeated TS locations (6 locations) captured the field mean within ±5% VSM during both the SMEX02 and SMEX05 campaigns. These 6 TS locations are marked in Figure 1. Overall, all the TS locations, in general, had lower temporal variability and RMSE values in SMEX05 compared to SMEX02. However, a few of the 18 repeated TS locations that were earlier dry in 2002 with respect to the field mean were wet in 2005 and vice versa.

[21] Similarly, in the WC12 field, during SMEX02, about 49% of the total 132 sampling locations (64 out of 132 locations) captured the field-averaged soil moisture within ±10% VSM. Approximately 67% of these 64 TS locations (i.e., 43 locations) captured the field mean within ±5% VSM. During SMEX05, because of a lack of human resources and other restrictions, sampling was done only along the two vertical transects, skipping the horizontal transect earlier sampled in SMEX02 (see Figure 1). Therefore, the total number of sampling locations in 2005 was reduced from 132 to 64. Of these 64 locations, about 28% (18 locations) and 55% (33 locations) captured the field mean soil moisture within ±05% and ±10% VSM, respectively. These 33 TS locations within ±10% VSM in SMEX05 included 14 of the 64 TS locations from SMEX02 with the same bias. About 36% of these repeated 14 TS locations (i.e., 5 out of 14 locations) captured the field mean within ±5% VSM. These common locations that were time stable during both SMEX02 and SMEX05 within the WC12 field are marked in Figure 1. Similar to the WC11 field, the repeated TS locations in WC12 also had lower temporal deviations and RMSE values in SMEX05 compared to SMEX02. Also, a few of the TS locations in WC12 were overestimating or underestimating the field mean soil moisture in 2005, opposite to that in 2002, while rest of the locations maintained their previous trend.

[22] Though the percentage of TS locations is higher in the WC12 field, WC11 still exhibits higher time stability as the temporal standard deviations and RMSE values at the TS locations in WC11 are comparatively lower. Another important observation is that the repeated TS locations during the 3 year period (2002–2005) are at moderate to high elevations in both the WC fields. Furthermore, the soil texture at these locations consists of either loam or clay loam soil. For elevation and soil maps of the WC fields, readers may refer to *Jacobs et al.* [2004]. Almost all the mean relative difference plots showed that the drier sampling locations have lower variability (smaller temporal deviation and smaller RMSE) compared to the wetter ones. This result is consistent with the findings of *Jacobs et al.* [2004] for SMEX02.

3.1.2. Watershed-Scale Time Stability Analyses With PSR Footprint-Scale Observations

[23] The PSR-estimated soil moisture content is quite low and almost uniform throughout the WC watershed in Iowa during SMEX02. Changes in soil moisture patterns are noticeable from 10 through 12 July 2002 after the rainfall event on 10 July 2002 (Figures 7a and 7b). Figure 8 shows the $\overline{\delta}_{i,j}$ values ranked from lowest to highest along with ±1 standard deviation bars and the RMSE values of the 84 pixels (resolution of 800 m × 800 m) of PSR in the WC watershed (see Figure 2). Nearly 21% of the pixels (18 of total 84 pixels) show strong time stability, with their pixel mean soil moisture value approximating the watershed mean within ±2% VSM. About 48% of the total pixels (41 of 84 pixels) captured the watershed mean within ±5% VSM, whereas nearly 80% (67 of 84 pixels) estimated the watershed mean within ±10% VSM. There are

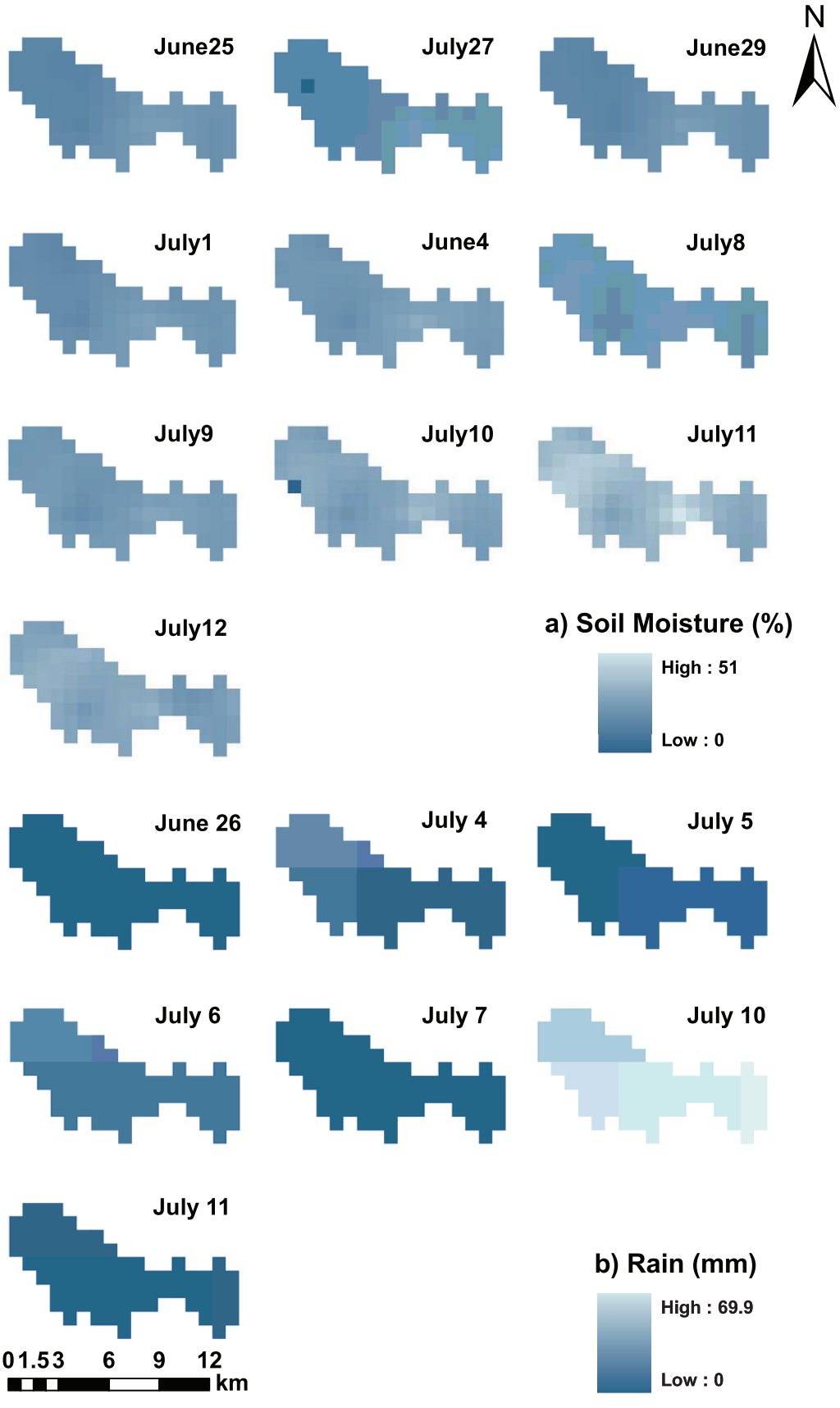

Figure 7. (a) The PSR-based soil moisture and (b) precipitation evolution map of the WC watershed (Iowa) during the SMEX02 campaign.

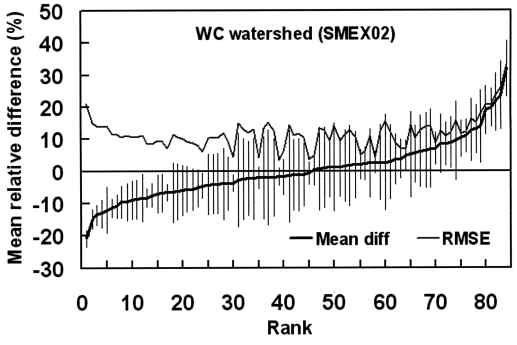

Figure 8. Rank-ordered mean relative difference with one standard deviation error bars and root-mean-square error for each PSR footprint in the WC watershed (Iowa) during SMEX02.

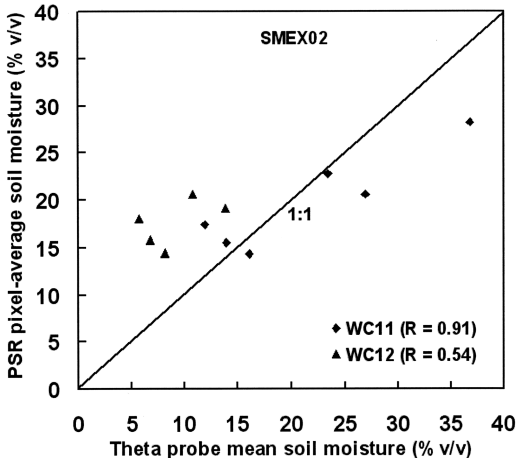

Figure 9. Comparison of theta probe–measured and the PSR-estimated mean volumetric soil moisture content of the WC11 and WC12 fields in the WC watershed (Iowa) during the SMEX02 campaign.

two pixels that exhibit the highest time stability with a ±0.5% bias and the lowest RMSE values (Figure 2a). From the digital elevation model (DEM) and slope maps, it is apparent that these two highest TS pixels are located at a higher elevation (311 m) with a low slope value (0.27%–0.28%). Thus, these two pixels seem to be located at hilltop within the watershed. One of the pixels is planted with soybean, while the other one has a grass cover. The soil texture of these two pixels is characterized by a high silt content (between 46%) but lower sand (29%) and clay (26%) contents (see Figures 2b–2e).

[24] A qualitative look at Figure 2e further shows that almost all the watershed pixels with higher TS characteristics (watershed mean soil moisture content within ±2% VSM bias) have a high silt content (46%–48%) and low sand (26%–29%) and clay (24%–26%) contents. Only four such TS pixels have a higher sand content (45%), whereas their silt and clay contents are 37% and 18%, respectively. From Figure 2b, some of the pixels exhibiting higher TS characteristics appear to be located in closer proximity to the watershed edge at low to high elevation. A possible reason for this could be attributed to the lateral drainage features of these pixels due to their role as a source instead of sink in the watershed. A few of the TS pixels are located within the watershed at intermediate elevations. Interestingly, these TS pixels do not have a definite crop type (Figure 2d). A few of them are soybean fields, while others have a corn or grass cover. These observations suggest that topography (elevation) and the soil parameters (such as percent silt and percent sand) could be the significant physical controls affecting the time stability of soil moisture at the 800 m × 800 m footprint scale as well as the point scale (see section 3.1.1).

3.1.3. PSR (Footprint Scale) Versus Theta Probe (Point Scale) Soil Moisture Data

[25] The PSR footprint containing the WC11 field has better TS characteristics (watershed mean soil moisture captured within ±5% VSM) compared to the PSR footprints overlapping with the WC12 field (watershed mean within ±10% VSM). This is somewhat similar to the findings obtained from the point-scale soil moisture data for the WC fields during SMEX02 and SMEX05, which show that WC11 exhibits higher time stability than the WC12 field. Figure 9 shows a comparison of the theta probe–measured and the PSR-derived soil moisture for the WC fields during SMEX02. Only those dates when measurements were recorded using both the instruments have been considered. The 1:1 line of the scatterplot shows that the PSR sensor estimates soil moisture content fairly well in the WC11 field ($R = 0.91$). However, in the WC12 field, the sensor consistently overestimates the moisture content compared to the in situ measurements ($R = 0.58$ only).

3.2. Little Washita Watershed, Oklahoma

3.2.1. Field-Scale Time Stability With Ground-Based Point-Scale Observations

[26] Figure 10 shows the time series of mean soil moisture along with their standard deviation for the three LW fields (LW03, LW13, and LW21) in the LW watershed, Oklahoma, during the SGP97 and CLASIC campaigns. As expected, the mean soil moisture content rises immediately after a precipitation event and then continues to decrease afterward throughout the dry down phase in all the fields. The soil moisture variability trend appears to be somewhat similar within the LW03 and LW13 fields during the experimental period interspersed with various rainfall events (Figures 10a and 10b). This may be due to the fact that both LW03 and LW13 are rangeland fields with a rolling topography. However, the variability in LW03 is higher than that of LW13 and LW21, which may be due to the difference in their characteristics dominant soil types. LW03 has sandy loam soil, whereas both LW13 and LW21 have silt loam. The soil moisture condition of the LW21 field is almost constant during CLASIC as the weather conditions were predominantly wet during the 3 week long campaign. Also, during SGP97, soil moisture variability within the same field rises slightly during the beginning of the drying phase and then remains almost constant for the rest of the experimental period marked with intermittent rainfall. This may be attributed to the fact that LW21 has a somewhat flat topography, and thus, soil moisture variability is mostly soil controlled.

[27] During SGP97, LW13 seems to exhibit higher TS characteristics with lower temporal deviation and lower

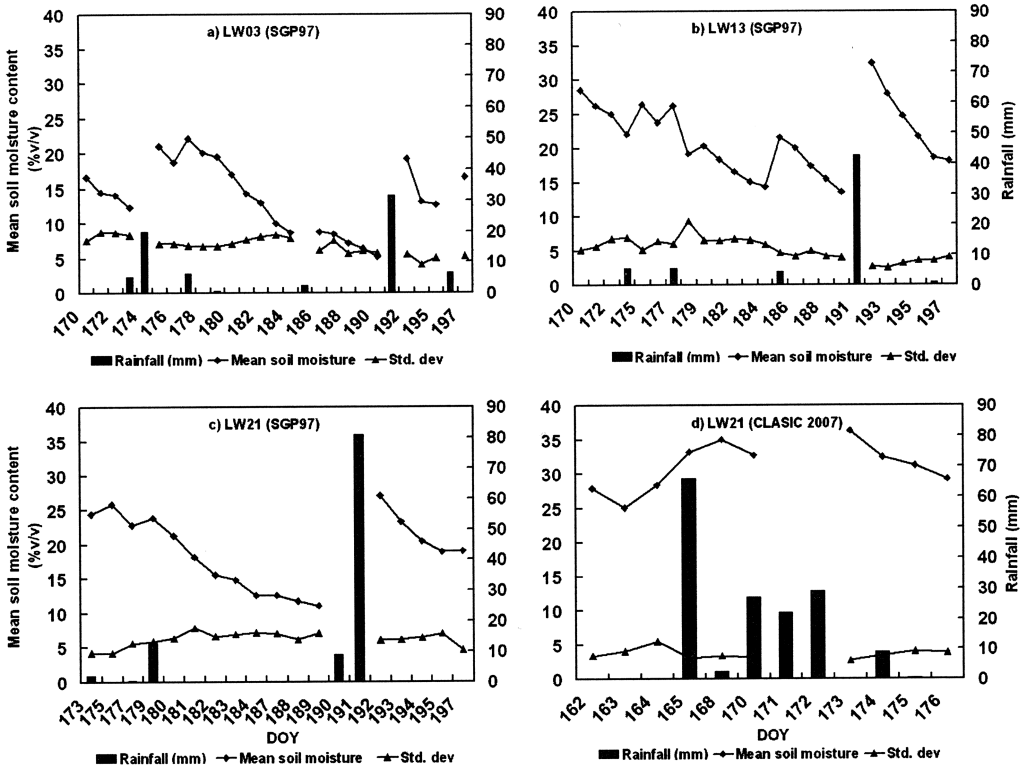

Figure 10. Mean and standard deviation of volumetric soil moisture content of fields (a) LW03, (b) LW13, and (c) LW21 during SGP97 and (d) the LW21 field during the CLASIC campaign in the LW watershed (Oklahoma).

RMSE values compared to fields LW03 and LW21 (Figures 11a–11c). LW21 exhibited the worst TS features, with TS locations ($\overline{\delta}_{i,j} \approx 0$) showing high temporal variability with large standard deviation error bars. Of a total of 49 sampling locations, about 25%, 39%, and 29% of the locations captured the field average soil moisture with a $\pm 10\%$ bias in LW03, LW13, and LW21, respectively. About 8%, 9%, and 8% of these TS locations captured the field mean within

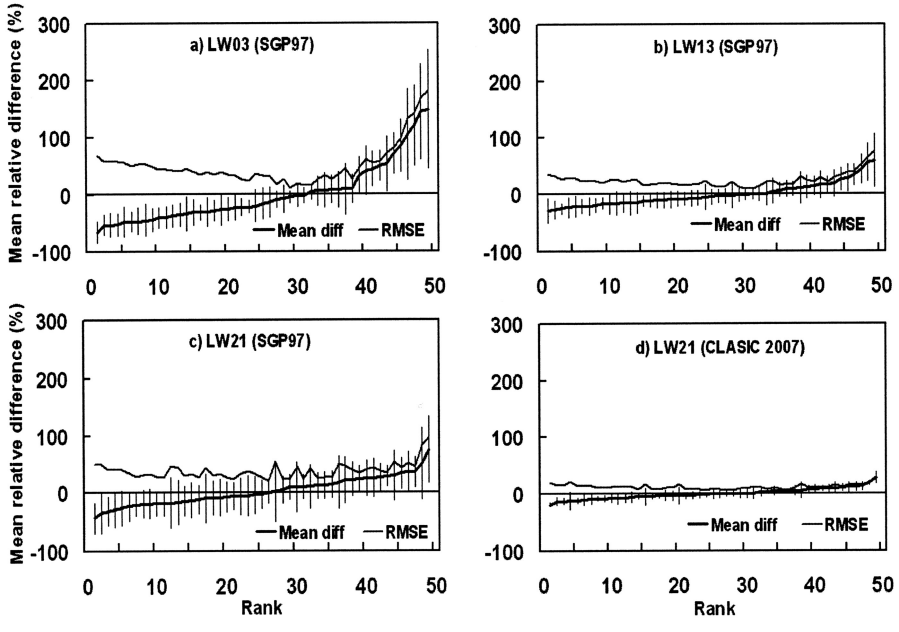

Figure 11. Rank-ordered mean relative difference with one standard deviation error bars and root-mean-square error for each sampling point in fields (a) LW03, (b) LW13, and (c) LW21 during SGP97 and (d) the LW21 field during the CLASIC campaign in the LW watershed (Oklahoma).

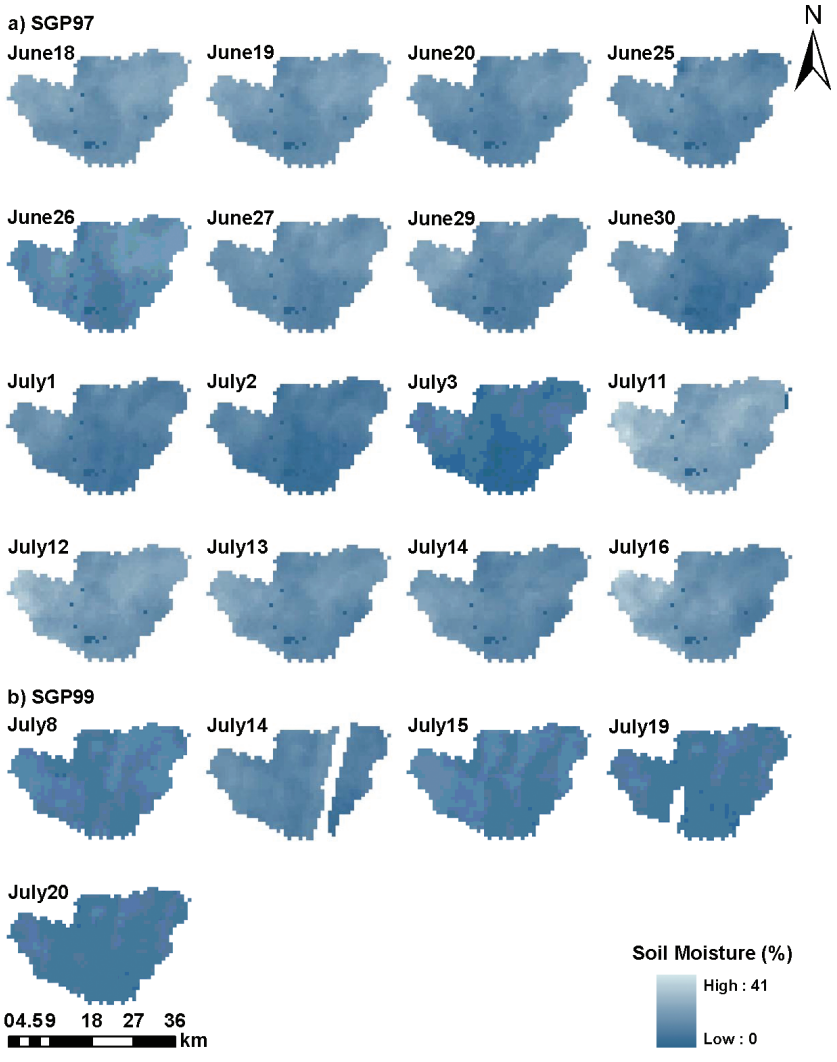

Figure 12. Soil moisture evolution map estimated from the ESTAR data within the LW watershed (Oklahoma) during the (a) SGP97 and (b) SGP99 campaigns.

±5% VSM in LW03, LW13, and LW21, respectively. In LW03, few of the sampling locations, which are wetter with respect to the field mean, are subjected to large temporal fluctuations. Furthermore, the drier sampling locations showed smaller temporal variability with smaller error bars compared to the wetter locations in the LW03 field. We made similar observations in the WC fields of the WC watershed (see section 3.1.1). For a detailed description regarding time stability characteristics of the LW fields during the SGP97 campaign, readers may refer to *Mohanty and Skaggs* [2001]. Furthermore, comparisons show that 10 of the 14 TS locations estimating the field mean soil moisture within ±10% VSM bias in LW21 during SGP97 were also time stable during CLASIC (Figure 11d). These locations that maintained their time stability during both SGP97 and CLASIC are shown in Figure 3.

3.2.2. Watershed-Scale Time Stability With ESTAR Footprint-Scale Observations

[28] The ESTAR-derived watershed mean soil moisture content as well as its temporal fluctuations is higher during SGP97 compared to SGP99 (Figures 12). However, the ESTAR data for SGP99 are sparse compared to the SGP97 data set. Therefore, it is not possible to make any inferences regarding the temporal variability in the watershed mean moisture values during SGP99. The overall soil moisture conditions are drier during SGP99 than during the SGP97 campaign. The rank-ordered $\overline{\delta}_{i,j}$ within ±1 standard deviation and their RMSE values for the ESTAR data sets are shown in Figure 13. During SGP97, approximately 28% of the pixels (269 out of 969 pixels) captured the watershed mean soil moisture within ±10% VSM, whereas in SGP99, nearly 33% of the pixels (165 out of 980 pixels) estimated the watershed mean within ±10% bias. About 13% (131 out of 969) and 17% (165 out of 980) of the pixels captured the watershed mean within ±5% VSM during SGP97 and SGP99, respectively. During SGP99, the temporal variations are comparatively lower than SGP97, with higher variability among the drier pixels than the wetter ones, similar to SGP97. Furthermore, investigations show about 114 common TS pixels capturing the watershed mean within ±10% VSM during both SGP97 and SGP99. Figure 14a shows the locations of these 114 repeated TS pixels

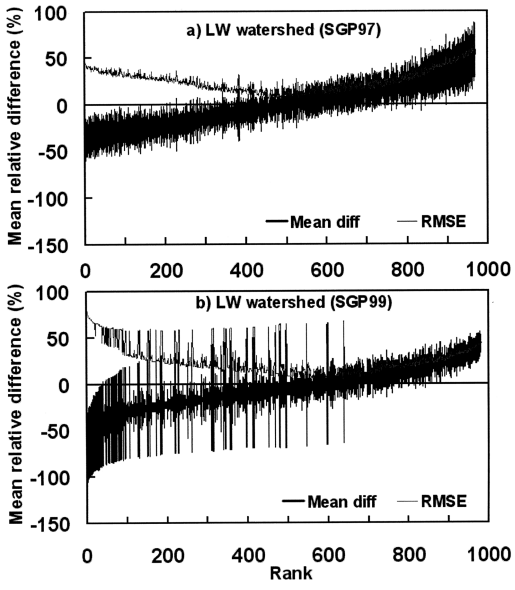

Figure 13. Rank-ordered mean relative difference with one standard deviation error bars and root-mean-square error for each ESTAR footprint in the LW watershed (Oklahoma) during the (a) SGP97 and (b) SGP99 campaigns.

overlaid on the DEM of the LW watershed. Of these 114 common TS pixels, 31 pixels capture the watershed mean soil moisture with a ±5% bias during both SGP97 and SGP99. However, it should be noted that since the RS data for SGP99 is temporally sparse, it is difficult to compare and make any definite inference regarding the long-term TS characteristics of these pixels within the LW watershed. Figure 14b shows the slope map of the LW watershed containing the most TS pixels that captured the watershed mean moisture content within ±1% VSM during the SGP97 and SGP99 campaigns (note that these pixels are not repeated TS locations during SGP97 and SGP99). It is evident that these pixels exhibiting higher time stability (within ±1% VSM) are mostly located at low to intermediate elevations in close proximity to the northeastern and southwestern edges of the watershed, with few of them scattered in the central region of the watershed. This is similar to the observations made at the WC watershed in Iowa during SMEX02, where the higher TS pixels (within ±2% VSM) are mostly at low to high elevation near the watershed edge (see section 3.1.2). A closer examination of the results shows that most of these TS pixels have moderate to high slope values. This suggests that slope could also be another factor besides elevation controlling the TS behavior of the pixels (800 m × 800 m) in this study watershed. These findings corroborate to the results of *Jawson and Niemann* [2007], who conducted an empirical orthogonal function (EOF) analysis using the SGP97 (ESTAR) data set to study the spatiotemporal variations in large-scale soil moisture patterns. In their study, they concluded that slope had moderate correlations with the primary EOFs for both the spatial and temporal soil moisture anomalies.

[29] Furthermore, analysis shows that these watershed pixels with higher TS characteristics have either higher silt content (≈47%) along the northeastern edge or higher sand content (≈56%) along the southwestern edge of the study watershed (see Figure 4d and Table 3). We made similar observations in the case of the WC watershed as well (see section 3.1.2). A qualitative look at Figures 4e–4f shows that a particular crop cover does not dominate among the TS pixels, although the number of pixels having pasture or rangeland covers is certainly higher than the rest during years 1997 and 1999. This may be attributed to the fact that the watershed was mostly covered with pastures or rangelands during both SGP97 and SGP99. Thus, similar to the WC watershed in Iowa, in the LW watershed, both topography (elevation and slope) and soil parameters (percent silt and percent sand) appear to be controlling the TS behavior of soil moisture at both point and footprint scales.

3.2.3. Factors Controlling Time Stability of Footprint-Scale Soil Moisture

[30] The one-way ANOVA tests were conducted for exploring the relationships between physical properties of the PSR footprints and their mean relative difference within the WC watershed during SMEX02. In addition, similar tests were conducted using the standard deviation of the relative difference to examine whether the observed variability of time stability is related to the physical parameters of the sampling footprints (see Table 4). The five physical properties of the RS footprints used in the analysis are percent clay, percent sand, soil texture, topography (based on combination of elevation and slope), and LULC. The geophysical data sets were aggregated or disaggregated to a cell size of 800 m × 800 m to match with the resolution of the sensor footprints. Percent clay and percent sand were both categorized using range of values from the CONUS soils database, whereas soil texture was categorized using loam and silt clay types. Topography was categorized using DEM-derived information regarding hillslope position. The DEM of the watershed was extracted from the GTOPO30 data (resolution of 1 km × 1 km) developed by the U.S. Geological Survey (USGS). Landscape positions were categorized on the basis of the degree of slope for each footprint as hilltop (slope 0%–0.45% with zero flow accumulation), depression (slope 0%–0.45% with flow accumulation), mild slope (0.45%–0.88%), and high slope (>0.88%) in the WC watershed. LULC included alfalfa, corn, grass, soybean, trees, and urban areas.

[31] ANOVA results for the mean relative differences show that the soil moisture time stability of the PSR footprints can be differentiated on the basis of soil properties, topography, and LULC. Tests using the standard deviation of the relative differences make it apparent that of the five physical attributes, the observed variability of time stability of the footprints can be differentiated on the basis of percent clay, percent sand, and topography. Compared to LULC, soil properties and topography are better able to discern the TS characteristics of the footprints. It is interesting to see that although percent clay, percent sand, and soil texture are correlated, the first two soil properties are better able to discern the TS features of the footprints compared to the soil texture. Figure 15 shows the mean relative difference of the PSR pixels categorized by the soil parameters (percent clay, percent sand, and soil texture), topography, and LULC during SMEX02. It is evident that none of the soil textures are able to identify the pixels that are close to mean relative difference (i.e., $\overline{\delta}_i = 0$). The 95%

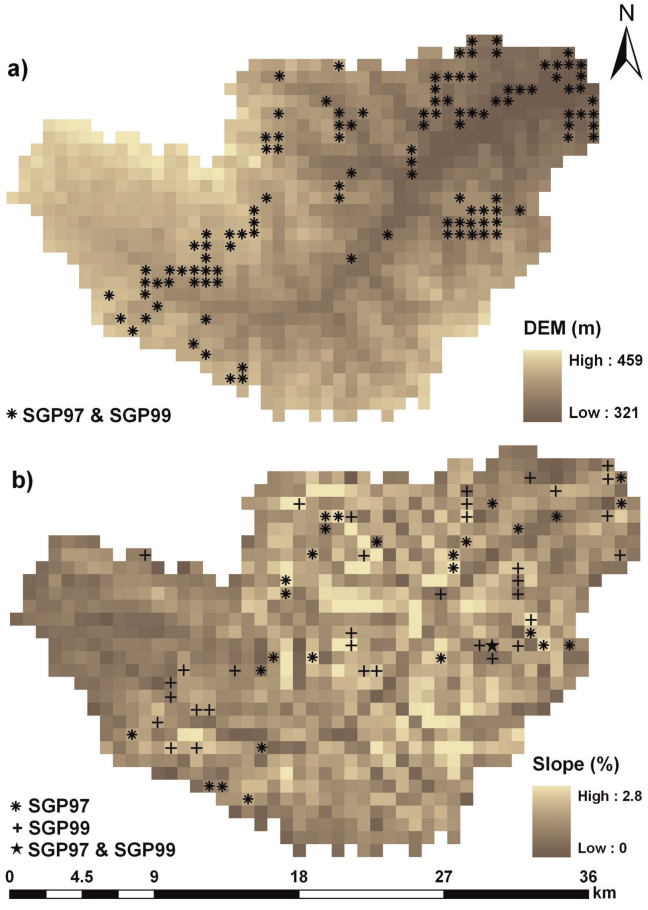

Figure 14. DEM and slope map of the LW watershed (Oklahoma) showing the location of the ESTAR pixels that were time stable within (a) ±10% VSM during both SGP97 and SGP99 and (b) ±1% VSM during the SGP97 and SGP99 campaigns. Note that the ESTAR pixels in Figure 14a are repeated TS locations during the SGP97 and SGP99 campaigns.

confidence intervals show a consistent wet bias for the loam soils and a dry bias for the silt clay soils. Furthermore, the pixels having loam soil texture with high sand (45%) but low clay (18%) content consistently overestimated the watershed mean soil moisture. On the other hand, the pixels with silt clay texture having equal amounts of clay and sand (26%) contents consistently underestimated the watershed mean. The transition from wet to dry bias occurs at about 24% clay and 29% sand, which closely matches with the watershed average percentage of clay (24%) and sand (31%). Overall, the best soil indicator of soil moisture time stability is the pixel with loam soil texture having 24% clay and 29% sand. In terms of topography, the hilltops (slope ~0%–0.45%) show the best TS features, with their respective mean relative differences close to zero (i.e., $\overline{\delta}_i = 0$). This result matches with the finding of our previous qualitative analysis (using the DEM and slope maps), where it was apparent that the two highest TS pixels were located at

Table 4. *F* Values for Tests of Difference in Mean Values by Sampling Property for the PSR- and the ESTAR-Based Soil Moisture Measurements Within the WC Watershed (SMEX02) and the LW Watershed (SGP97)[a]

	PSR Data (SMEX02)		ESTAR Data (SGP97)	
Remote Sensing Pixel Property	$\overline{\delta}_{i,j}$	$\sigma(\delta_{i,j})$	$\overline{\delta}_{i,j}$	$\sigma(\delta_{i,j})$
Percent clay	<0.001***	0.009**	<0.001***	<0.001***
Percent sand	<0.001***	0.009**	<0.001***	<0.001***
Soil texture	<0.001***	0.118 (NS)	<0.001***	<0.001***
Topography	0.036*	0.004**	<0.001***	<0.001***
Land use–land cover	0.039*	0.717 (NS)	<0.001***	0.026**

[a]The analysis of variance test examines the mean relative difference ($\overline{\delta}_{i,j}$) and standard deviation of relative differences ($\sigma(\delta_{i,j})$). NS indicates nonsignificant difference at the 0.05 significance level, and asterisks indicate the following: single asterisk, significance at the 0.05 significance level; two asterisks, significance at the 0.01 significance level; three asterisks, significance at the 0.001 significance level. PSR, Polarimetric Scanning Radiometer; ESTAR, Electronically Scanned Thin Array Radiometer.

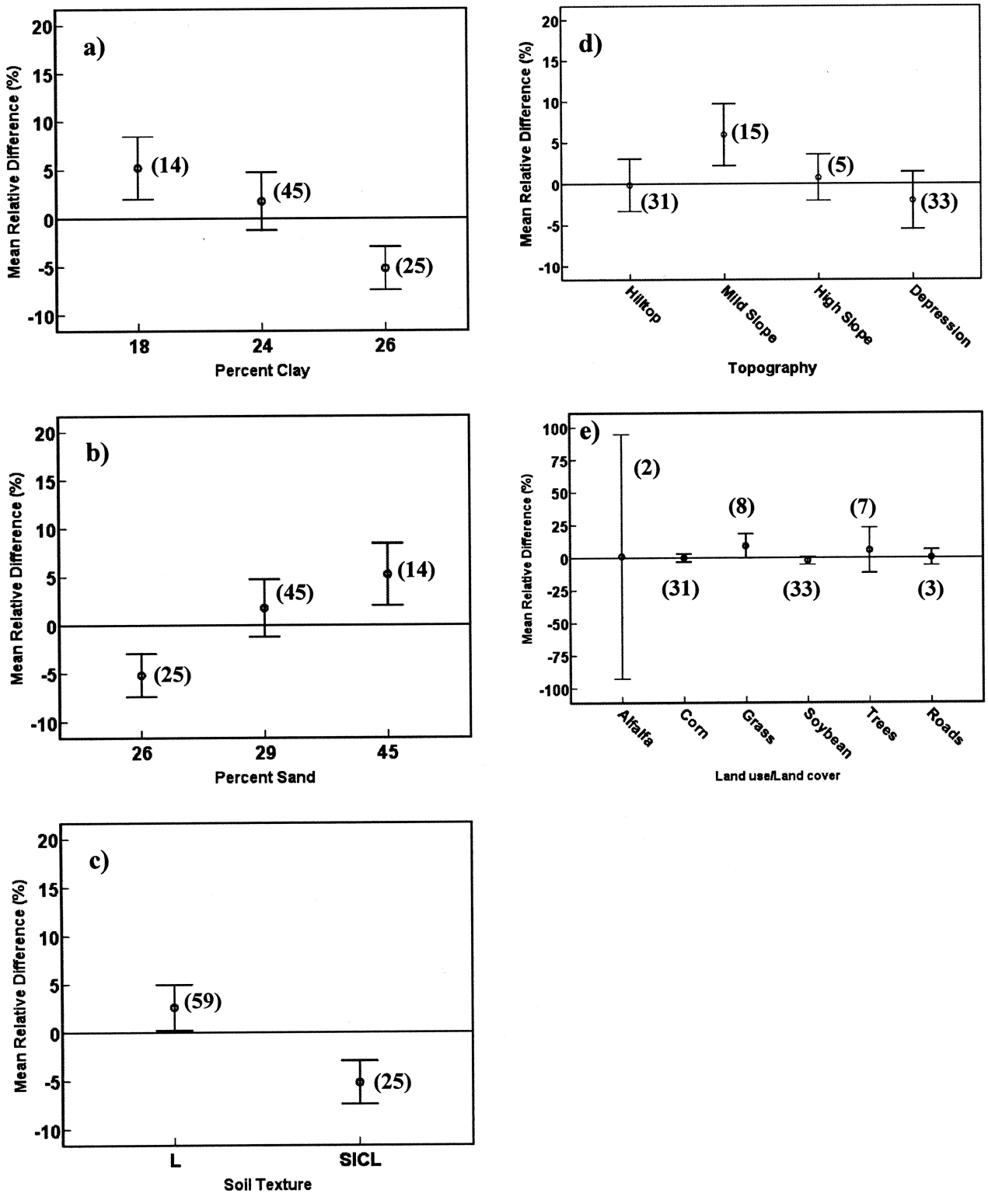

Figure 15. Mean relative difference and 95% confidence interval by soil parameters: (a) percent clay, (b) percent sand, (c) soil texture, (d) topography, and (e) LULC in the WC watershed (Iowa) during the SMEX02 campaign. The number of pixels with each physical parameter is shown in parenthesis.

a higher elevation (~311 m) with a low slope value (0.27%–0.28%). From Figure 15e, pixels having corn and soybean crop cover show better time stability compared to the rest. The Pearson coefficients for the WC watershed in Table 5 show a significant correlation between the mean relative difference ($\overline{\delta_{i,j}}$) and the three soil parameters (percent clay, percent sand, and soil texture) characterizing the PSR pixels.

Table 5. Pearson Correlation Coefficients for the WC Watershed (Iowa) and the LW Watershed (Oklahoma)[a]

	$\overline{\delta}_{i,j}$	Percent Clay	Percent Sand	Soil Texture	Topography	Land Use–Land Cover
			WC Watershed			
$\overline{\delta}_{i,j}$	1	−0.348**	0.313**	−0.401**	−0.138	−0.026
Percent clay	−0.348**	1	−0.991**	0.591**	−0.626**	−0.225*
Percent sand	0.313**	−0.991**	1	−0.478**	−0.030	0.257*
Soil texture	−0.401**	0.591**	−0.478**	1	−0.135	0.075
Topography	−0.138	0.007	−0.030	−0.135	1	−0.228*
Land use–land cover	−0.026	−0.225*	0.257*	0.075	−0.228*	1
			LW Watershed			
$\overline{\delta}_{i,j}$	1	0.320**	−0.701**	0.037	0.023	0.167**
Percent clay	0.320**	1	−0.679**	−0.506**	0.051	0.025
Percent sand	−0.701**	−0.679**	1	−0.069*	−0.036	−0.131**
Soil texture	0.037	−0.506**	−0.069*	1	−0.040	0.057
Topography	0.023	0.051	−0.036	−0.040	1	−0.009
Land use–land cover	0.167**	0.025	−0.131**	0.057	−0.009	1

[a]Asterisks indicate the following: single asterisk, correlation is significant at the 0.05 significance level; two asterisks, correlation is significant at the 0.01 significance level.

[32] Similar analyses were performed using the ESTAR data set for the LW watershed during the SGP97 campaign. Soil texture within the LW watershed was categorized using loam, sand, sandy loam, and silt loam types. Landscape positions were categorized as hilltop (0%–0.93% with zero flow accumulation), depression (0%–0.93% with flow accumulation), mild slope (0.93%–1.85%), and high slope (>1.85%). LULC of the ESTAR pixels was categorized as shown in Figure 16e. Results for the mean relative differences show that the soil moisture time stability of the ESTAR pixels can be differentiated on the basis of soil properties, topography, and LULC. Also, the observed variability of time stability of the footprints can be differentiated on the basis of the above-mentioned five physical properties of the ESTAR footprints. The pixels with sandy loam soil texture having 10% clay and 60% sand (with a consistent dry bias) are better indicators of time stability of the pixels. Also, the pixels with loam soil texture having 15% clay and 37% or 41% sand (with a consistent wet bias) are better indicators of the time stability phenomena (see Figures 16a–16c). The watershed averages of clay and sand contents are 13% and 44%, respectively. Figure 16d shows that the pixels with mild slope (0.93%–1.85%) are the best indicators of TS features of the ESTAR pixels. Also, a particular LULC type does not dominate the TS characteristics of the ESTAR footprints (Figure 16e). Correlation analysis shows a significant relation between the mean relative difference ($\overline{\delta}_{i,j}$) and percent clay and percent sand for the ESTAR pixels (see LW watershed data in Table 5).

4. Conclusions

[33] Analyses of both in situ (point scale) and passive microwave RS (sensor footprint scale) soil moisture data from the SMEX02 and SMEX05 field campaigns conducted in the WC watershed in Iowa show that soil properties (i.e., percent silt, percent sand, and soil texture) and topography (elevation and slope) are significant physical parameters that jointly control the spatiotemporal evolution and variability and TS features of soil moisture. At the field scale, the WC11 field exhibited higher time stability and lower temporal variation compared to the WC12 field during the 3 year span (2002–2005). The common TS points during the 3 year period (2002–2005) were mostly located at moderate to high elevations in both fields. Soil texture at these locations consists of either loam or clay loam soil. Presence of tile drainage features in the WC12 field affected the soil moisture variability within the field. Crop rotation during SMEX02 and SMEX05 seems to have had an effect on the soil moisture variability in the WC11 field. At the RS footprint scale, the ANOVA tests show that percent clay and percent sand are better able to discern the TS features of the footprints compared to the soil texture in the WC watershed. Overall, the best soil indicator of soil moisture time stability at the footprint scale is the loam soil texture. Furthermore, the hilltops (slope ∼0%–0.45%) showed the best TS characteristics, with their respective mean relative differences closer to zero (i.e., $\overline{\delta}_i = 0$). The two most TS pixels are located at a higher elevation (∼311 m), with a slope value of 0.27%–0.28%, within the WC watershed. Finally, a particular LULC type does not seem to influence the footprint-scale soil moisture time stability.

[34] In the LW watershed, Oklahoma, our analyses of both field-based and RS soil moisture data obtained from SGP97 and SGP99 indicate that both soil properties (percent silt, percent sand, and soil texture) and topography (elevation and slope) are significant physical controls jointly affecting the spatiotemporal evolution and time stability of soil moisture at both point and footprint scales, similar to the observations made in the WC watershed in Iowa. At the field scale, the silt loam field (LW13) was more time stable than the sandy loam field (LW03) and the silt loam field (LW21). Field LW21, with flat topography, showed least TS features compared to both LW03 and LW13, which have gently rolling topography. At the footprint scale, ANOVA results show that the pixels with sandy loam soil texture having 10% clay and 60% sand and those with loam soil texture having 15% clay and 37% or 41% sand are better indicators of the time stability phenomena in the LW watershed. In terms of the hillslope position, mild slopes (0.93%–1.85%) are the best indicators of TS features of the ESTAR footprints. Also, a particular LULC type does not affect the TS characteristics of the footprints. These findings can prove beneficial when designing long-term soil moisture monitoring networks and planning

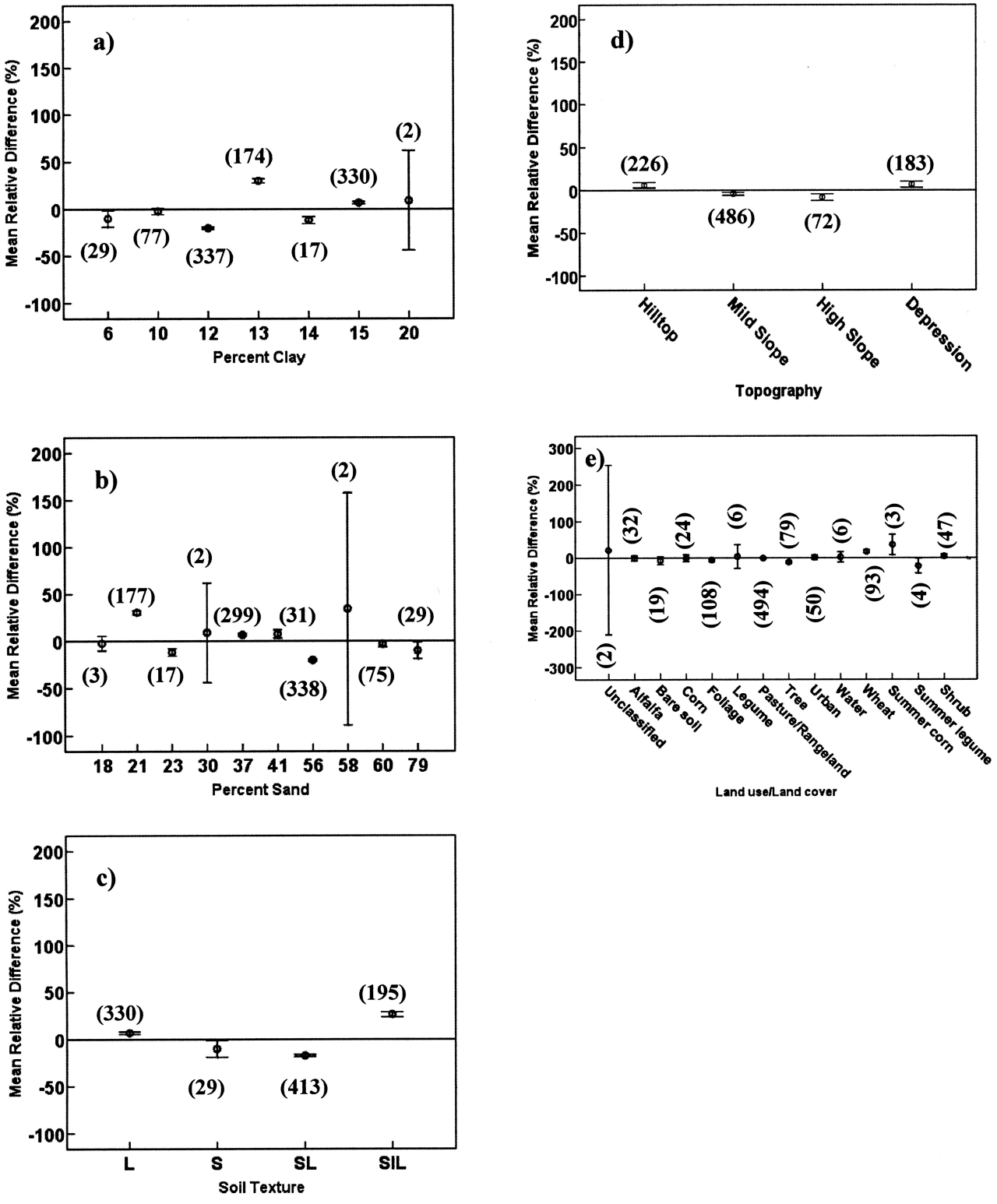

Figure 16. Mean relative difference and 95% confidence interval by soil parameters: (a) percent clay, (b) percent sand, (c) soil texture, (d) topography, and (e) LULC in the LW watershed (Oklahoma) during the SGP97 campaign. The number of pixels with each physical parameter is shown in parenthesis.

intensive, short-term field campaigns for validating airborne- or satellite-based RS soil moisture data.

[35] **Acknowledgments.** The research was funded by NASA THP grants NNX08AF55G and NNX09AK73G and NSF (CMG/DMS) grant 0621113. We would like to acknowledge the partial support of the USGS for this work. The authors also wish to thank the team of scientists and student participants involved in data collection during the SGP97, SGP99, SMEX02, SMEX05, and CLASIC campaigns.

References

Bindlish R., T. J. Jackson, A. J. Gasiewski, M. Klein, and E. G. Njoku (2005), Soil moisture mapping and AMSR-E validation using the PSR in SMEX02, *Remote Sens. Environ.*, *103*(2), 127–139.

Choi M., and J. M. Jacobs (2007), Soil moisture variability of root zone profiles within SMEX02 remote sensing footprints, *Adv. Water Resour.*, *30*(4), 883–896.

Cosh M. H., T. J. Jackson, R. Bindlish, and J. H. Prueger (2004a), Watershed scale temporal and spatial stability of soil moisture and its role in validating satellite estimates, *Remote Sens. Environ.*, *92*(4), 427–435.

Cosh M. H., J. R. Stedinger, and W. Brutsaert (2004b), Variability of surface soil moisture at the watershed scale, *Water Resour. Res.*, *40*, W12513, doi:10.1029/2004WR003487.

Cosh M. H., T. J. Jackson, S. Moran, and R. Bindlish (2008), Temporal persistence and stability of surface soil moisture in a semi-arid watershed, *Remote Sens. Environ.*, *112*, 304–313.

De Troch F. P., P. A. Troch, Z. Su, and D. S. Lin (1996), Application of remote sensing for hydrologic modeling, in *Distributed Hydrologic Modeling*, edited by M. B. Abbott and J. C. Refsgaard, pp. 165–192, Kluwer Acad., Dordrecht, Netherlands.

Entin J. K., A. Robock, K. Y. Vinnikov, S. E. Hollinger, S. X. Liu, and A. Namkhai (2000), Temporal and spatial scales of observed soil moisture variations in the extratropics, *J. Geophys. Res.*, *105*(D9), 11,865–11,877.

Famiglietti J. S., J. A. Devereaux, C. A. Laymon, T. Tsegaye, P. R. Houser, T. J. Jackson, S. T. Graham, M. Rodell, and P. J. van Oevelen (1999), Ground-based investigation of soil moisture variability within remote sensing footprints during the Southern Great Plains 1997 (SGP97) Hydrology Experiment, *Water Resour. Res.*, *35*(6), 1839–1851.

Famiglietti J. S., D. Ryu, A. A. Berg, M. Rodell, and T. J. Jackson (2008), Field observations of soil moisture variability across scales, *Water Resour. Res.*, *44*, W01423, doi:10.1029/2006WR005804.

Grayson R. B., and A. W. Western (1998), Towards areal estimation of soil water content from point measurements: Time and space stability of mean response, *J. Hydrol.*, *207*, 68–82.

Jackson T. J. (1993), Measuring Surface soil-moisture using passive microwave remote-sensing, III, *Hydrol. Processes*, *7*(2), 139–152.

Jackson T. J., and D. E. Le Vine (1996), Mapping surface soil moisture using an aircraft-based passive microwave instrument: Algorithm and example, *J. Hydrol.*, *184*, 85–99.

Jackson T. J., and T. J. Schmugge (1995), Surface soil-moisture measurement with microwave radiometry, *Acta Astronaut.*, *35*(7), 477–482.

Jacobs J. M., B. P. Mohanty, E.-C. Hsu, and D. Miller (2004), SMEX02: Field scale variability, time stability and similarity of soil moisture, *Remote Sens. Environ.*, *92*, 436–446.

Jawson S. D., and J. D. Niemann (2007), Spatial patterns from EOF analysis of soil moisture at a large scale and their dependence on soil, land-use, and topographic properties, *Adv. Water Resour.*, *30*(3), 366–381.

Kachanoski R. G., and E. Dejong (1988), Scale dependence and the temporal persistence of spatial patterns of soil-water storage, *Water Resour. Res.*, *24*, 85–91.

Kim G., and A. P. Barros (2002a), Space-time characterization of soil moisture from passive microwave remotely sensed imagery and ancillary data, *Remote Sens. Environ.*, *81*(2-3), 393–403.

Kim G., and A. P. Barros (2002b), Downscaling of remotely sensed soil moisture with a modified fractal interpolation method using contraction mapping and ancillary data, *Remote Sens. Environ.*, *83*(3), 400–413.

Martinez-Fernandez J., and A. Ceballos (2003), Temporal stability of soil moisture in a large-field experiment in Spain, *Soil Sci. Soc. Am. J.*, *67*, 1647–1656.

Mohanty B. P., and T. H. Skaggs (2001), Spatio-temporal evolution and time-stable characteristics of soil moisture within remote sensing footprints with varying soil, slope, and vegetation, *Adv. Water Resour.*, *24*, 1051–1067.

Mohanty B. P., P. J. Shouse, and M. T. van Genuchten (1998), Spatio-temporal dynamics of water and heat in a field soil, *Soil Tillage Res.*, *47*(1-2), 133–143.

Mohanty B. P., T. H. Skaggs, and J. S. Famiglietti (2000), Analysis and mapping of field-scale soil moisture variability using high-resolution, ground-based data during the Southern Great Plains 1997 (SGP97) Hydrology Experiment, *Water Resour. Res.*, *36*(4), 1023–1031.

Mohanty B. P., P. J. Shouse, D. A. Miller, and M. T. van Genuchten (2002), Soil property database: Southern Great Plains 1997 Hydrology Experiment, *Water Resour. Res.*, *38*(5), 1047, 10.1029/2000WR000076.

Njoku E. G., T. J. Jackson, V. Lakshmi, T. K. Chan, and S. V. Nghiem (2003), Soil moisture retrieval from AMSR-E, *IEEE Trans. Geosci. Remote Sens.*, *41*(2), 215–229.

Ott L. (1997), *An Introduction to Statistical Methods and Data Analysis*, Duxbury, North Scituate, Mass.

Piepmeier J. R., and A. J. Gasiewski (2001), High-resolution passive polarimetric microwave mapping of ocean surface wind vector fields, *IEEE Trans. Geosci. Remote Sens.*, *39*(3), 606–622.

Ryu D., and J. S. Famiglietti (2005), Characterization of footprint-scale surface soil moisture variability using Gaussian and beta distribution functions during the Southern Great Plains 1997 (SGP97) Hydrology Experiment, *Water Resour. Res.*, *41*, W12433, doi:10.1029/2004WR003835.

Schmugge T. J. (1998), Applications of passive microwave observations of surface soil moisture, *J. Hydrol.*, *212–213*, 188–197.

Ulaby F. T., P. C. Dubois, and J. van Zyl (1996), Radar mapping of surface soil moisture, *J. Hydrol.*, *184*, 57–84.

Vachaud G., A. P. Desilans, P. Balabanis, and M. Vauclin (1985), Temporal stability of spatially measured soil-water probability density-function, *Soil Sci. Soc. Am. J.*, *49*(4), 822–828.

Yoo C. (2002), A ground validation problem of remotely sensed soil moisture data, *Stochastic Environ. Res. Risk Assess.*, *16*(3), 175–187.

A. V. M. Ines, International Research Institute for Climate and Society, Earth Institute at Columbia University, 61 Rte. 9W, Palisades, NY 10964, USA. (ines@iri.columbia.edu)

J. M. Jacobs, Department of Civil Engineering, University of New Hampshire, Durham, NH 03824, USA. (jennifer.jacobs@unh.edu)

C. Joshi and B. P. Mohanty, Department of Biological and Agricultural Engineering, Texas A&M University, 2117 TAMU, 201 Scoates Hall, College Station, TX 77843, USA. (bmohanty@tamu.edu)